# Ultra stable all-fiber telecom-band entangled photon-pair source for turnkey quantum communication applications

**Chuang Liang, Kim Fook Lee, Todd Levin, Jun Chen, and Prem Kumar**

*Center for Photonic Communication and Computing, Electrical Engineering and Computer Science Department, Northwestern University, 2145 Sheridan Road, Evanston, IL 60208*
liang@ece.northwestern.edu

**Abstract:** We demonstrate a novel alignment-free all-fiber source for generating telecom-band polarization-entangled photon pairs. Polarization entanglement is created by injecting two relatively delayed, orthogonally polarized pump pulses into a piece of dispersion-shifted fiber, where each one independently engages in four-photon scattering, and then removing any distinguishability between the correlated photon-pairs produced by each pulse at the fiber output. Our scheme uses a Michelson-interferometer configuration with Faraday mirrors to achieve practically desirable features such as ultra-stable performance and turnkey operation. Up to 91.7% two-photon-interference visibility is observed without subtracting the accidental coincidences that arise from background photons while operating the source at room temperature.



**OCIS codes:** (270.0270) Quantum optics; (190.4370) Nonlinear optics, fibers; (999.9999) Quantum communications; (060.0060) Fiber optics and optical communications.

## References and links

1. N. Gisin, G. Ribordy, W. Tittel, and H. Zbinden, "Quantum cryptography," Rev. Mod. Phys. **74**, 145–195 (2001).
2. D. Bouwmeester, J.-W. Pan, K. Mattle, M. Eibl, H. Weinfurter, and A. Zeilinger, "Experimental quantum teleportation," Nature **390**, 575–578 (1997).
3. P. G. Kwiat, K. Mattle, H. Weinfurter, A. Zeilinger, A. V. Sergienko, and Y. H. Shih, "New High-Intensity Source of Polarization-Entangled Photon Pairs," Phys. Rev. Lett. **75**, 4337–4340 (1995).
4. M. Fiorentino, P. L. Voss, J. E. Sharping, and P. Kumar, "All-fiber photon-pair source for quantum communication," Photon. Technol. Lett. **14**, 983–985 (2002).
5. X. Li, P. L. Voss, J. E. Sharping, and P. Kumar, "Optical-Fiber Source of Polarization-Entangled Photons in the 1550 nm Telecom Band," Phys. Rev. Lett. **94**, 053601 (2005).
6. H. Takesue and K. Inoue, "Generation of polarization-entangled photon pairs and violation of Bell's inequality using spontaneous four-wave mixing in a fiber loop," Phys. Rev. A **70**, 031802 (2004).
7. X. Li, J. Chen, P. L. Voss, J. Sharping, and P. Kumar, "All-fiber photon-pair source for quantum communications: improved generation of correlated photons," Opt. Express **12**, 3737–3744 (2004).
8. J. G. Rarity, J. Fulconis, J. Duligall, W. J. Wadsworth, and P. S. J. Russell, "Photonic crystal fiber source of correlated photon pairs," Opt. Express **13**, 534–544 (2005).
9. J. E. Sharping, J. Chen, X. Li, and P. Kumar, "Quantum-correlated twin photons from microstructure fiber," Opt. Express **12**, 3086–3094 (2004).
10. J. Fan, A. Dogariu, and L. J. Wang, "Efficient generation of correlated photon pairs in a microstructure fiber," Opt. Lett. **30**, 1530–1532 (2005).
11. P. Kumar, M. Fiorentino, P. L. Voss, and J. E. Sharping, "All-fiber photon-pair source for quantum communications," U. S. Patent No. 6,897,434 (2005).
12. X. Li, C. Liang, K. F. Lee, J. Chen, P. L. Voss, and P. Kumar, "An integrable optical-fiber source of polarization-entangled photon pairs in the telecom band," Phys. Rev. A **73**, 052301 (2006).
13. Y. Takushima, S. Yamashita, K. Kikuchi, and K. Hotate, "Single-frequency and polarization-stable oscillation of Fabry-Perot fiber laser using a nonpolarization-maintaining fiber and an intracavity etalon," Photon. Technol. Lett. **8**, 1468–1470 (1996).

#70561 - $15.00 USD Received 3 May 2006; accepted 10 July 2006

14. A. Muller, T. Herzog, B. Huttner, W. Tittel, H. Zbinden, and N. Gisin, "Plug and play systems for quantum cryptography," Appl. Phys. Lett. **70**, 793–795 (1997).
15. X. Li, P. L. Voss, J. Chen, J. E. Sharping, and P. Kumar, "Storage and long-distance distribution of telecommunications-band polarization entanglement generated in an optical fiber," Opt. Lett. **30**, 1201–1203 (2005).
16. C. Liang, K. F. Lee, J. Chen, and P. Kumar, "Distribution of fiber-generated polarization entangled photon-pairs over 100 km of standard fiber in OC-192 WDM environment," postdeadline paper, Optical Fiber Communications Conference (OFC'2006), paper PDP35.
17. H. Takesue, "Long-distance distribution of time-bin entanglement generated in a cooled fiber," http://xxx.lanl.gov/abs/quant-ph/0512163.
18. K. F. Lee, J. Chen, C. Liang, X. Li, P. L. Voss, and P. Kumar, "Generation of high-purity telecom-band entangled-photon pairs in dispersion-shifted fiber," Opt. Lett. **31**, 1905–1907 (2006).

## 1. Introduction

Quantum entanglement is a key resource in most quantum-communication protocols such as quantum cryptography [1] and quantum teleportation [2]. Therefore, an efficient, stable, and easy-to-operate source of entanglement is highly desirable for practical quantum communications. Spontaneous parametric down conversion in $\chi^{(2)}$ crystals [3] is widely used for generating entangled photon pairs in laboratory environments. However, its free-space and non-telecom-band nature greatly limits its practical applicability in long-distance quantum communications, although those might be overcome by dedicated coupling and frequency-conversion techniques at the cost of source efficiency.

Recently, a new method of creating entangled photon pairs has been proposed and demonstrated [4-12], which utilizes four-photon scattering (FPS) in fused silica fiber through its $\chi^{(3)}$ (Kerr) nonlinearity. The fiber nature of this source brings advantages such as no coupling loss to the transmission fiber, spatial purity of the guided modes, and telecom-band operation. Thus this type of source is particularly suitable for long-distance quantum-communication applications and has attracted a lot of research interest. Here is a brief description of the method with an example for creating polarization-entangled photon pairs. Two orthogonally polarized pump pulses are prepared with a relative delay and fixed relative phase $\varphi_p$. They are injected into a piece of optical fiber where each pump pulse independently engages in FPS. In this process two pump photons at frequency $\omega_p$ scatter through the Kerr nonlinearity to create time-energy entangled daughter signal-idler photon pairs at frequencies $\omega_s$ and $\omega_i$, respectively, such that $2\omega_p=\omega_s+\omega_i$. The pump wavelength is chosen close to the zero-dispersion wavelength of the fiber in order to achieve phase matching for best FPS efficiency. The generated signal-idler photon pair inherits polarization property of the parent pump due to the isotropic nature of the $\chi^{(3)}$ nonlinearity in silica fiber. Before leaving the source fiber, the FPS processes originating from each pump pulse with definite polarization are coherently combined while removing information such as the relative time delay. This makes the created photon pairs from the two FPS processes indistinguishable from each other and polarization entanglement is established. As in other entangled-photon sources, pump power can be tuned to a level such that with high probability only one photon pair is emitted from the two FPS processes.

There are two major schemes in the literature for realizing such fiber-based polarization entanglement. In Ref. 5 a free-space Michelson interferometer is employed for preparing 30 ps relative delay between the two orthogonally polarized 5-ps-duration pump pulses. This time delay is erased by passing the signal-idler photon pairs, which are generated in a 300-m-long fiber Sagnac loop made of dispersion-shifted fiber (DSF), through 20 m of polarization maintaining fiber. To maintain a fixed relative phase between the pump pulses, sophisticated phase tracking and locking is needed. In addition, fiber-birefringence induced polarization fluctuations need to be carefully compensated before sending the photon pairs through the polarization maintaining fiber for accurately removing the time delay. Hence this scheme is too complicated for practical usage. A counter-propagating scheme is proposed in Ref. 11 and

#70561 - $15.00 USD Received 3 May 2006; accepted 10 July 2006

demonstrated in Refs. 6 and 12 wherein a piece of DSF is connected to two output ports of a polarization beam splitter (PBS). Linearly polarized pump pulses at 45° are injected through one input port of the PBS so that the DSF is simultaneously pumped with the decomposed orthogonally polarized pump pulses in both clockwise and counter-clockwise directions. Photon pairs generated from the two counter-propagating FPS processes are recombined upon arrival at the PBS, thus establishing polarization entanglement in the photon pairs that emerge from the other port of the PBS. No phase tracking is needed for proper operation. However, a polarization control paddle is still needed to compensate the environmentally driven polarization fluctuations that occur inside the DSF on time scales of hours. Thus this scheme is still not suitable for real-world practice where reliable turnkey operation is highly desired.

Here we propose and demonstrate a new alignment-free fiber-based scheme for creating telecom-band polarization-entangled photon pairs. Long-term polarization and/or phase fluctuations are automatically compensated. The scheme utilizes fiber-pigtailed optical components which have been fully integrated for turnkey operation.

## 2. Details of the Scheme and Experimental Configuration

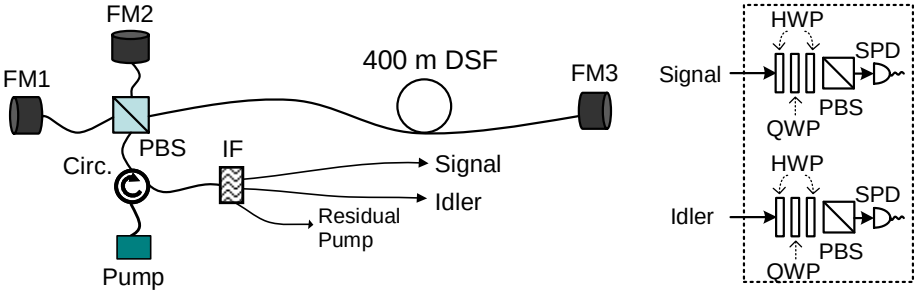


Fig. 1. (a) Scheme for the turnkey polarization-entangled photon-pair source. (b) Photon-pair receiver for characterizing the source. FM1-3, fiber Faraday mirrors; Circ., circulator; IF, fiber interference filters; DSF, dispersion-shifted fiber; PBS, polarization beam splitter; HWP, half-wave plate; QWP quarter-wave plate; SPD, single-photon detector.

Our scheme is shown in Fig. 1(a). The system's principal axes are defined by a four-port fiber PBS. An optical pump-pulse train is prepared at 45° linearly polarized relative to the principal axes and is injected into a fiber circulator which has the basic property of transmitting incident light between its three ports in a successive fashion: light incident on port one is passed to port two and light that returns back into port two is then passed to port three. To avoid unfavorable polarization rotation of the pump pulses, a polarization-maintaining fiber circulator can be used for bringing the pump pulses to the input port of the PBS. At the output ports of the PBS, each 45° linearly-polarized pump pulse is decomposed into horizontally- and vertically-polarized components $P_H$ and $P_V$, respectively, with a relative phase $\varphi_p$ equal to zero.

$P_V$ is reflected and guided to a Faraday mirror (FM1) at the start of its itinerary: PBS→FM1→PBS→FM3→PBS→FM2→PBS. A Faraday mirror is a non-reciprocal optical element which produces a reflection with a state-of-polarization (SOP) that is orthogonal to the input SOP. Thus, uncontrolled polarization rotations occurring along the incident path are automatically compensated on the return path. Such Faraday mirrors have previously been used in classical as well as quantum applications. See, for example, Ref. 13 for a classical application and Ref. 14 for a quantum application. In our case, $P_V$ becomes horizontally polarized upon returning to the PBS after reflection from FM1. It then passes through the PBS and enters a 400-m piece of DSF where the FPS process takes place. Similarly, $P_H$ starts it journey PBS→FM2→PBS→FM3→PBS→FM1→PBS by going to FM2. It then arrives back at the PBS vertically polarized and reflects to enter the DSF. A small length difference between the paths to FM1 and FM2 are intentionally designed so that a time delay, which is

#70561 - $15.00 USD Received 3 May 2006; accepted 10 July 2006

much greater than the pump-pulse duration, is introduced between the arrival times of $P_H$ and $P_V$ at the DSF.

In the DSF, $P_H$ and $P_V$ independently engage in FPS processes and create signal-idler photon pairs. Note that $P_H$ and $P_V$ experience almost the same insertion loss before entering into the DSF; thus the two FPS processes have almost the same efficiency. As mentioned above, the daughter signal-idler photon pairs are co-polarized with the parent pump pulses. With the use of FM3, birefringence-induced polarization fluctuations on the light in the DSF between PBS and FM3 are also automatically compensated. In addition, the polarization states of the two pump pulses and the daughter photon pairs are rotated by 90° when they arrive back at the PBS. Hence, $P_V$ and the photon pairs generated from it are directed towards FM2 while $P_H$ and its daughter photon pairs travel to FM1. It is easy to see that the information on the birth time of the newly-born photon pairs is automatically erased when $P_H$ and $P_V$, along with their daughter photon pairs, are recombined at the PBS traveling backward through the input port. Upon emerging from the PBS the circulator then directs them away from the pump towards the receivers. With a properly set pump power, the signal-idler photon pairs are emitted in one of the maximally-entangled states: $|H\rangle_s|H\rangle_i+|V\rangle_s|V\rangle_i$. It is also important to point out that the pump pulses travel through the DSF twice in this scheme because of FM3. Both $P_H$ and $P_V$ follow a symmetric path through the system. It is this symmetry and the use of Faraday mirrors which automatically compensate any long-term polarization and/or phase fluctuations that enable an ultra-stable and alignment-free source of polarization entanglement. After passing through the circulator, the signal-idler photon pairs are separated from the residual pump by fiber interference filters, which are then ready for use in various quantum communication applications [15-17].

We have built a proof-of-principle prototype to demonstrate this scheme. It uses a 400-m piece of DSF with a zero-dispersion wavelength near 1556 nm. A 50-MHz repeated ~5-ps-duration pump pulse train is obtained by sending ~100 fs optical pulses emitted by a fiber laser through cascaded 200-GHz-spacing ITU-grid fiber interference filters centered at 1555.95 nm. A fiber polarizer is used to set the incident polarization at 45° relative to the principal axes. Signal/idler photon pairs are collected by 200-GHz-spacing filters centered at 1550.92 nm and 1561.01 nm, respectively. We evaluate the quality of this photon-pair source by examining two-photon interference (TPI) with joint photon-counting measurements on the generated signal-idler photon pairs.

Figure 1(b) depicts details of the measurement apparatus. The signal and idler photons are spatially separated and then directed to different polarization analyzers. Each analyzer set contains a HWP-QWP-HWP polarization rotator, PBS, and a single-photon detector (SPD). After calibrating the system with the first HWP and the QWP, we measure TPI by recording coincidence counts as a function of the relative angle $\theta$ between orientations of the 2$^{nd}$ HWP in each analyzer. The created polarization entanglement will give rise to a TPI fringe on the coincidence counting rate in the form of $\cos^2\theta$, while the number of photon counts in individual analyzers is a constant for different angle settings. To detect the telecom-band photons, we operate Epitaxx EPM239BA InGaAs/InP avalanche photo diodes in gated Geiger mode (electrically reverse biased slightly above the breakdown voltage) as single-photon detectors (SPDs) (see Ref. 4). Although the entangled-photon source is operated at 50 MHz, the effective sampling rate of the whole system is limited by the SPDs, which have quantum efficiencies of about 20% and dark count probabilities of ~$10^{-3}$ counts/gate, to a gate-pulse rate of 785 kHz.

### 3. Experiment Results

The results of TPI measurements are shown in Fig. 2 (a)–(c), where the solid lines are the $\cos^2\theta$ fitting curves. Solid diamonds are the number of measured coincidences between the signal and idler photon counts, where only the contributions from the detector dark counts have been subtracted. Empty squares are the number of signal-photon counts and the shaded triangles are the number of idler-photon counts. The relative polarization angle $\theta$ is changed

#70561 - $15.00 USD Received 3 May 2006; accepted 10 July 2006

by rotating the 2nd HWP in the idler's path while fixing the orientation of the HWP in the signal's path. Performances for different pump powers in the DSF are recorded.

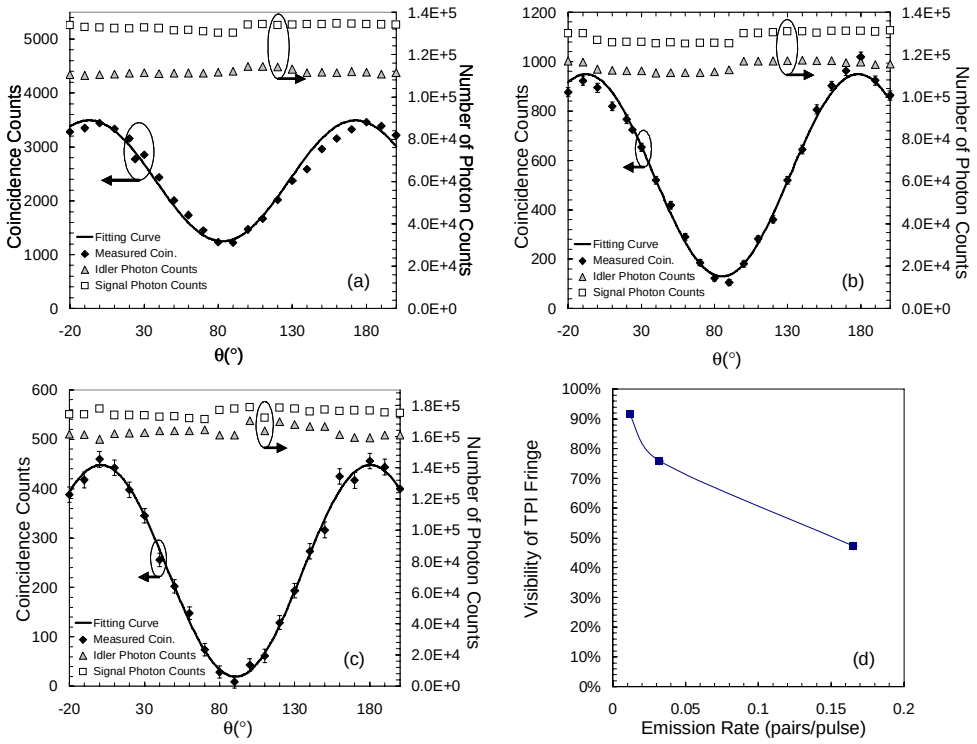


Fig. 2. Experimental results with different average pump powers coupled in the DSF: (a) 111 μW; (b) 42.3 μW; (c) 27.5 μW. (d): TPI visibility versus photon-pair emission rate. The curve has no meaning; it is shown only to guide the eye.

An average pump power of about 110 μW in the DSF, which corresponds to approximately 440 mW peak power, is used for the set of data shown in Fig. 2(a), where each data point is acquired by sampling for 10 s at 785 kHz. Due to the high peak power used, the number of photon-pairs produced inside the DSF during each pump pulse is around 0.376. This number is usually termed as the production rate for estimating the efficiency of the FPS process inside the DSF. For quantum communication applications, the number of photon pairs actually emitted from the source, for instance after the filters in Fig. 1(a), is of more practical relevance. We name this number as the emission rate, which is 0.165 for the set of data in Fig. 1(a). As shown, a TPI fringe with visibility of 47.3% arises in the joint measurements, while almost constant numbers of photon counts are obtained in individual measurements of either the signal or idler photons. The difference in the signal and idler photon counts mainly comes from the different detection efficiencies in the two analyzers. Similarly, in Fig. 2(b), a TPI visibility of 75.9% is observed at a 0.032 pairs/pulse emission rate when the average pump power is adjusted to 42.3 μW (169 mW peak power) inside the DSF. The integration time is increased to 30 s for acquiring each point in this data set. As shown in Fig. 2(c), a TPI visibility of 91.7% is measured at a 0.012 pairs/pulse emission rate when the average pump power in the DSF is further reduced to 27.5 μW (110 mW peak power). Due to further reduction of the pump power, a longer sampling time of 60 s is used for each point in this set of data. We note from Fig. 2(a-c) that the ratio between the signal and idler photon counts changes slightly with pump power. This may be due to the slightly different nonlinear coefficients at the signal and idler wavelengths together with the quadratic vs. linear pump-power dependence of the FPS and Raman gains, respectively.

#70561 - $15.00 USD Received 3 May 2006; accepted 10 July 2006

The dependence of the TPI visibility with emission rate is summarized in Fig. 2(d). At higher pump powers, the probability of creating multiple photon pairs per pulse is high. In addition, there is higher probability for the pump photons to leak through the filters. Both these effects lead to increased accidental-coincidence counts, thus reducing the TPI visibility as observed in Fig. 2(a). At low pump powers we believe it is the spontaneous Raman scattering that is responsible for the majority of background photons which prevent us from observing perfect TPI visibility. Studies have shown that the contribution of Raman-scattered background photons can be reduced by cooling the fiber [17, 18]. Similar behavior as the trend line for the TPI visibility versus the emission rate shown in Fig. 2(d) is also reported in Ref. 18, where significantly more data taken using the counter-propagating scheme was presented in the low emission-rate regime. The only difference is that in Ref. 18, the curves are plotted as coincidence to accidental-coincidence ratio versus the pump power. In summary, the TPI results obtained with this turnkey prototype are comparable with those obtained previously using other fiber-based schemes. Finally, no alignment adjustment was needed during the course of the above measurements. To further ascertain the stability of the source, we intentionally disturbed the DSF and the fibers between the PBS and FM1/FM2 during the experiment. No performance penalty was observed.

## 4. Conclusion

In conclusion, we have introduced a novel all-fiber scheme for producing telecom-band polarization-entangled photon pairs. A double-pass Michelson-interferometer configuration is used with Faraday mirrors that automatically compensate system drifts such as polarization and phase fluctuations introduced by environmental perturbations on the fibers. With minimal engineering effort, this scheme could lead to an ultra-stable turnkey polarization-entangled photon-pair source which can be fully integrated for practical use. With our prototype source, up to 91.7% TPI visibility is demonstrated without subtracting the Raman-induced accidental coincidences under room-temperature operation. This much TPI visibility would lead to a violation of the CHSH form of Bell's inequality as shown in Ref. 18. Finally, we note that this scheme also has the advantages present in the previously reported counter-propagating scheme [12]: i) the cross-polarized spontaneous Raman scattering is automatically suppressed and ii) all the polarization-entangled photon pairs created by the pump are collected.

This work has been supported by DARPA under grant No. F30602-01-2-0528.

#70561 - $15.00 USD Received 3 May 2006; accepted 10 July 2006